THE STUDY OF THE PROPERTIES OF NANOMATERIALS

Original article
https://doi.org/10.15828/2075-8545-2022-14-3-198-204

In-situ transmission electron microscopy investigation on the evolution of Pt nanocrystals in oxidizing and reduing atmospheres

Qinglin Liu, Huanyu Ye, Zhihong Zhang, Rongming Wang*,
University of Science and Technology Beijing, Beijing 100083, China
* Corresponding author: e-mail: rmwang@ ustb.edu.cn

ABSTRACT: Metal nanocrystals exhibit unique properties due to their high surface-to-volume ratio and have great potential for applications in the fields of electronics, magnetics, optics and catalysis. However, their high specific surface area leads to easy coarsening in operation, which may greatly degrade their performances, especially when they are exposed to various chemical environments or at high temperatures. Therefore, the direct visualization of nanocrystals' structural evolution when they are coarsening is crucial to gain insight into the mechanism and develop more effective means to improve the size stability of nanocrystals. In this work, we investigated the structural evolution of Pt nanocrystals with sizes of ~ 4 nm on SiN_x film in both oxidizing and reducing atmospheres at a moderate temperature (300°C) in the aberration-corrected environmental transmission electron microscopy (ETEM). The sizes of nanocrystals remain almost unchanged when annealed in the oxygen atmosphere with volatile PtO_x formation on the surface, hindering nanocrystals sintering and leading to Pt loss. On the other hand, obvious coarsening of nanocrystals resulting from Ostwald-ripening and nanocrystal migration and coalescence was observed in the reducing atmosphere. Our findings reveal the dynamic structural evolution of nanocrystals in different atmospheres and provide possible ways to improve the size stability of nanocrystals.

KEYWORDS: nanocrystal, in-situ transmission electron microscopy (TEM), structural evolution, size stability, atmosphere.

ACKNOWLEDGMENT: This work was supported by Beijing Natural Science Foundation (Grant No. 2212034), the National Natural Science Foundation of China (Nos. 51971025 and 12034002), and the Fundamental Research Funds for the Central Universities (06108248, 06500235).

FOR CITATION: Qinglin Liu, Huanyu Ye, Zhihong Zhang, Rongming Wang. In-situ transmission electron microscopy investigation on the evolution of Pt nanocrystals in atmosphere. *Nanotechnologies in Construction*. 2022; 14(3): 198–204. https://doi.org/10.15828/2075-8545-2022-14-3-198-204. – EDN: DRKXKU

INTRODUCTION

The size of metal nanocrystals is one of the key factors determining their physical and chemical properties and applications in the fields of electronics, magnetics, optics, and catalysis.[1-5] Many strategies have been proposed to prepare small nanocrystals successfully, whereas their high specific surface area also leads to easy coarsening in operation which may significantly degrade their performance, especially when they are exposed to some chemical environments or at high temperatures.[6–8] Therefore, the size control of nanocrystals is of great significance not only in the synthesis process but also in the specific operational environment.

The prerequisite of realizing the size control is to achieve a detailed understanding of the influence factors and mechanisms that govern the nanocrystal coarsening. Extensive ex-situ experiments have been carried out, which characterize the structure and size of the nanocrystals before and after the treatment in certain environments to deduce the physical process of coarsening, providing a lot of useful information to understand the coarsening.[9, 10] However, there are always inconsistencies between different experimental results and deviations of experimental results from predicted models. Therefore, ex-situ experiments could not give an unambiguous physical picture of coarsening.[11, 12] In-situ techniques could provide an ideal platform to perform direct observations of dynamic

structural evolution and properties changes in various surroundings.[13] Environmental transmission electron microscopy (ETEM) is one of the most effective in-situ techniques to study the nanocrystal shape, size and structures in various gas environments and can obtain real-time and dynamic evolution data at the atomic scale.[14–17]

In this work, we in-situ investigated the evolution of the Pt nanocrystals in both reducing and oxidizing atmospheres at a 300°C by ETEM. Several works have studied the coarsening phenomenon of Pt nanocrystals supported by oxide substrate and carbon in different gas atmospheres. In all these studies, the substrates can strongly interact with Pt nanocrystals or even react with them and thus influence their coarsening behaviors.[18–20] But the effects of substrates were always not taken into consideration when they discussed the results and thus inconsistent conclusions were obtained.[21] In this work, we selected SiN_x film as the substrate, which is chemically stable and inert, and thus it has negligible effects on coarsening.

Our in-situ TEM observation found that in the oxidizing atmosphere, a PtO_x shell may form on the surface of nanocrystals which can greatly restrain the migration and coarsening of the nanocrystal. Therefore, the nanocrystals annealed in O_2 exhibited high size stability. By contrast, the nanocrystals coarsened obviously when they were annealed in the reducing atmosphere where Ostwald-ripening, and migration and coalescence of nanocrystals occurred. Our direct observations of the dynamic evolutions of nanocrystal size and structure can give useful information to deeply understand the coarsening phenomenon of metal nanocrystals, and propose possible strategies to improve the size stability of nanocrystals.

METHODS AND MATERIALS

The ETEM FEI Titan G2 80-300 kV equipped with objective lens spherical aberration corrector was applied to investigate the evolution of Pt nanocrystals in different atmospheres. The Pt nanocrystals were prepared by heating the chloroplatinic acid (H_2PtCl_6) precursor at an elevated temperature in ETEM. In a typical experiment, 1 g H_2PtCl_6 (AR, Pt ⩾ 37.5%) was dissolved in 50 mL ethanol and dispersed onto a heating chip with SiN_x film. After being dried for 24 hours in vacuum, the H_2PtCl_6 crystals precipitated out on the SiN_x film and then were loaded at a heating holder. The sample loading area of the heating chip is 75 μm in diameter with 22 holes covered with porous SiN_x film, as shown in Fig. 1a–c. The temperature was elevated to 300°C with a heating rate of and then kept at 300°C for 2 hours. The 200 Pa 20% H_2/Ar and pure O_2 environments were applied respectively at different heating processes. The in-situ observation was recorded by a dynamic camera with 4096×4096 pixels under adjustable integration time from 0.1 to 5.0 s. Statistical analysis was carried out by OriginPro Learning Edition software. The statistical results were expressed as the mean standard deviation values and tested by t-test. The quantified average size for each set of data was confirmed to be a normal distribution. A p-value of < 0.05 was considered to be statistically significant.

RESULTS

The typical H_2PtCl_6 crystals precipitated out on SiN_x film at room temperature are shown in Fig. 1d. It is found that the H_2PtCl_6 crystals with a size of about 100 nm are more likely to form around the SiN_x film-free area. The zoom-in bright-filed image of the H_2PtCl_6 crystal reveals a nonuniform mass and diffraction contrast as shown in Fig. 1e. It is implied that the existence of crystal defects and depressed surface in the crystallite.

The corresponding H_2PtCl_6 crystal space group is $Fm\bar{3}m$ and stands along the [001] direction with exposed {100} facets as confirmed by the previous work.[17] The energy-dispersive X-ray spectroscopy (EDS) elemental mappings of H_2PtCl_6 crystal were obtained by scanning TEM (STEM) mode. As shown in Fig. 1f, g, the crystallite exhibits a uniform distribution of Pt and Cl elements.

Then we heated the system with a heating rate of 1.0 °C/s and then kept the temperature at 300°C for 2 hours in different atmospheres. In both the oxidizing and reducing gas environments, the H_2PtCl_6 precursor started to decompose and form Pt nanocrystals when the temperature was up to 270°C. The detailed process of decomposition of solid-phase H_2PtCl_6 precursor, the nucleation and early-stage growth of Pt nanocrystals have been studied in our previous work.[17] Here we intend to investigate the size stability of Pt nanocrystals in atmospheres, and so we focus on the size and structure evolution of Pt nanocrystals during the annealing process at 300°C.

The oxidizing atmosphere was applied by introducing 200 Pa O_2 to the ETEM. Fig. 2a displays the ETEM image acquired when the temperature just reached 300°C, showing the almost uniformly distributed Pt nanocrystals. The inserted statistical particle size distribution (PSD) shows a single-peak profile and most of the Pt nanocrystals are 2~5 nm in size. The calculated average size is 3.5±1.1 nm. Upon in-situ annealing in this oxidizing atmosphere for 60 min, the average nanocrystal size is found to remain nearly unchanged as shown in Fig. 2b, c. Besides, we can see the positions of the Pt nanocrystals barely change by comparing these images. These results imply that under this oxidizing environment (200 Pa O_2, 300°C), the nanocrystals can maintain their size and their diffusion on the substrate is largely hindered as well.

In the case of the reducing atmosphere, we introduced 200 Pa 20% H_2/Ar into the ETEM and followed the same experimental procedure. Fig. 2d shows the Pt nanocrystals at the beginning of annealing in the reducing gas. Most nanocrystals were in the size of 3~6 nm and some larger

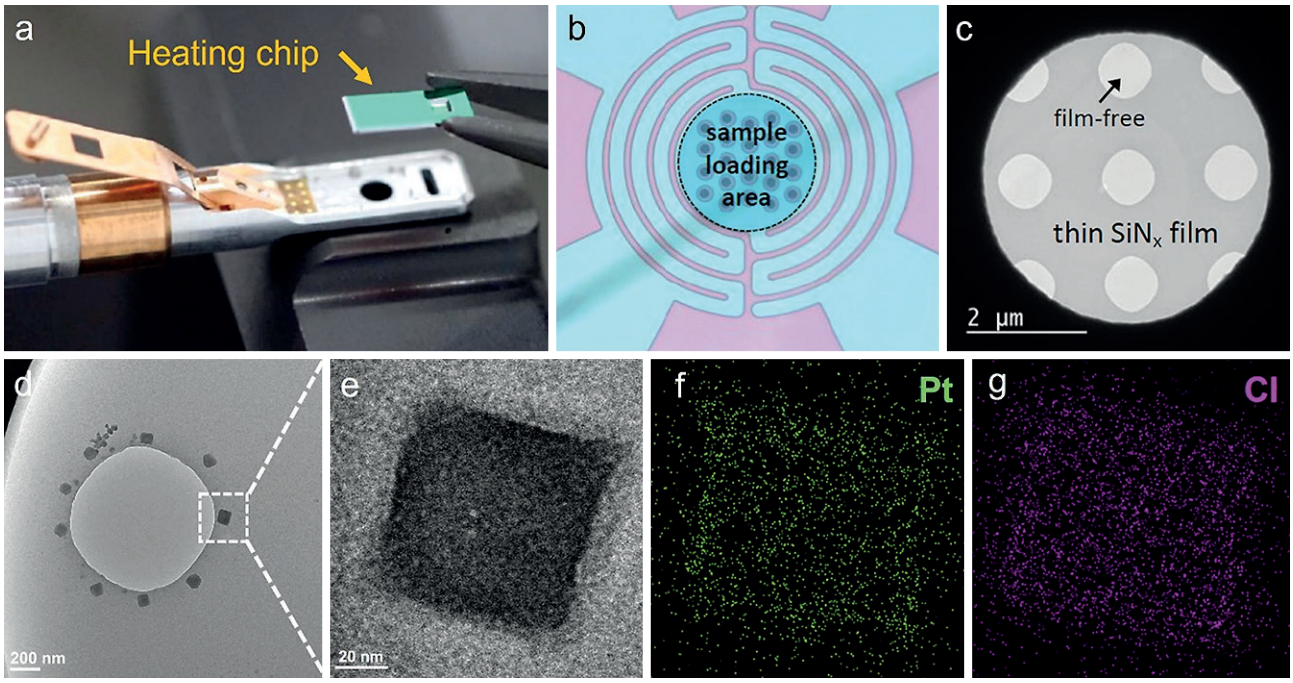

Fig. 1. **Scheme of the heating holder and heating chip (a); Morphology of sample loading area and thin SiN_x film of a heating chip (b, c); TEM images (d, e) and EDS mappings (f, g) of the H_2PtCl_6 crystal.**

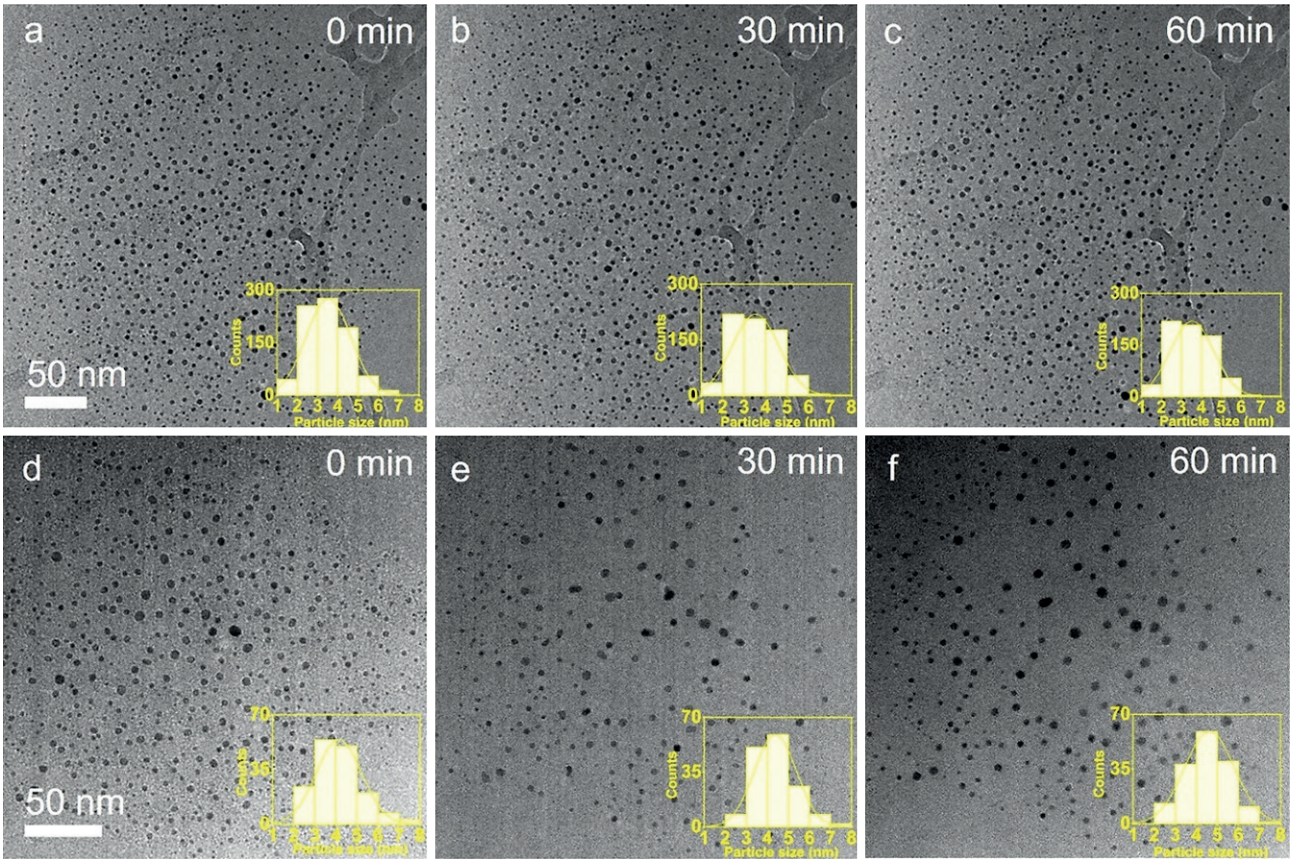

Fig. 2. **In-situ TEM images of Pt nanocrystals annealed in O_2 environment (a–c) and in H_2/Ar environment (d–f) for different annealing times. Inset: particle size distribution.**

nanocrystals can also be observed. The counted PSD still showed a single-peak profile, and the calculated average size of 150 counted nanocrystals was 4.1±1.0 nm. Compared with the nanocrystals treated in O_2, this larger average nanocrystal size indicates that nanocrystal coarsening may already occur in the preceding heating-up process in the reducing atmosphere. We also calculated the nanocrystal density before the annealing process, which was 9.1×10^{-3} n•nm^{-2}. After annealing for 30 min, the average nanocrystal size and density obviously changed (Fig. 2e). The calculated average size of nanocrystals was 4.4±1.0 nm with an increase of 7.3% and particle density was 5.2×10^{-3} n•nm^{-2}, which decreased by 42.9%. By the PSD results, we can find the proportion of nanocrystals with size in the range of 2~4 nm decreased from 51.2% (Fig. 2d) to 38.3% (Fig. 2e), while the one with a size larger than 5 nm increased from 19.2% to 23.4%. The ETEM image and statistical results indicate that after the 30 min annealing in the reducing atmosphere, the nanocrystals coarsened by Ostwald-ripening, where small nanocrystals were eaten by the larger ones. Also, we can observe in the ETEM image that two neighboring large nanocrystals migrated toward each other and coalesced (Fig. 2d,e). For the further 30 min annealing, the average size of nanocrystals increased a little by 12.2% and the nanocrystal density had hardly changed (Fig. 2f).

Above studies of the Pt nanocrystal coarsening phenomenon were performed over a large region that contained a large number of nanocrystals and by statistical results. We have achieved a primary understanding of the nanocrystal coarsening behaviors in both oxidizing and reducing atmospheres. Next, in order to get a deeper insight into the atomic structural evolution of the nanocrystal coarsening process, we applied in-situ high-resolution TEM (HRTEM) observation to reveal the atomic structural evolution of the nanocrystal coarsening process under O_2 and 20% H_2/Ar environments.

As shown in Fig. 3a-c, we traced three nanocrystals and recorded an in-situ HRTEM image under the 200 Pa O_2 at 300°C. The clear lattice fringes on the three particles can be identified as Pt {111} or {200} crystal planes. In addition, we found that there were several orientations in one nanocrystal (for example, the nanocrystal marked by the number 2, 2# nanocrystal), implying a polycrystalline structure as shown in Fig. 3a. 3# nanocrystal had a cashew-like morphology which may form by the aggregation of two nanocrystals during the heating stage. As the annealing proceeded, we found that there was an

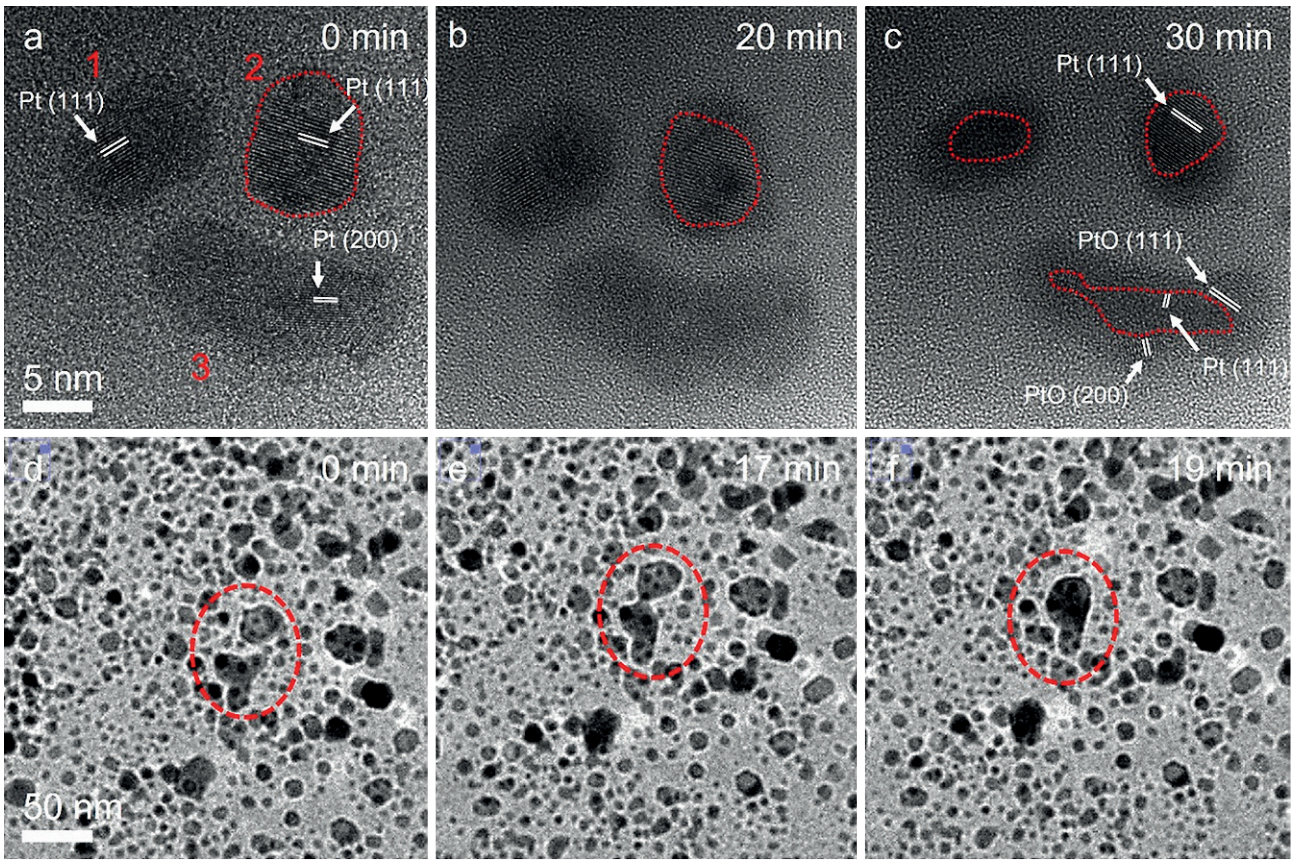

Fig. 3. **In-situ HRTEM images of Pt nanocrystals annealed in O_2 (a-c) and in H_2/Ar (d-f) for different times.**

amorphous shell structure with a weaker phase-contrast formed on the Pt nanocrystal surface (Fig. 3b) and further annealing led to the thickening and crystallizing of the shell structure (Fig. 3e). Fringes in the crystallized shell structure on 3# nanocrystal can be identified as the PtO {111} and {200} crystal planes (ICSD PDF#47-1171). Accordingly, we can speculate that the amorphous shell is also the Pt oxide, where the introduction of the O element into the Pt lattice obviously weakens the phase contrast.

It is worth noting that the coalescence and aggregation were not observed in this case, which can be ascribed to the Pt oxide formation on the nanocrystal surface. What's more, as the annealing continued, the nanocrystal size decreased a little (Fig. 3e), resulting from the volatility of Pt oxide.

We also recorded in-situ HRTEM images of Pt nanocrystals annealed under the 200 Pa 20% H_2/Ar at 300°C (Fig. 3d–f). The nanocrystals exhibited a specific shape morphology, different from those in O_2 environments. As we mentioned above, the Pt nanocrystals were more vulnerable to coarsening under the H_2/Ar environments. As marked with red dash circles in Fig. 3, a complete migration and coalescence process of nanocrystals was recorded and this behavior can be explained by coalescence and aggregation growth mechanisms. These results again confirmed the coarsening of Pt nanocrystals in the reducing atmosphere.

We further prolonged the annealing time in both oxidizing and reducing atmospheres and characterized the structure of the nanocrystals. After being annealed for 2 hours under O_2, some Pt nanocrystals were completely transformed into PtO_x nanocrystals, and some larger nanocrystals kept an obvious Pt/PtO_x core-shell structure as shown in Fig. 4a. The selected area electron diffraction (SAED) pattern in Fig. 4b revealed the coexistence of a variety of PtO_x crystal structures and pure Pt nanocrystal. The PtO#1 {111} (ICSD PDF#47-1171), PtO#2 {002} (ICSD PDF#42-0866), Pt_3O_4 {211} (ICSD PDF#21-1284) and Pt {200}{111} (ICSD PDF#04-0802) can be clearly identified. The HRTEM image shows the sub-nanometer-thick PtO_x shell was formed on the Pt nanocrystal surface, and the thinnest region only contained a few atomic layers (Fig. 4c). The two nanocrystals in the lower-left corner are attached but not merged under

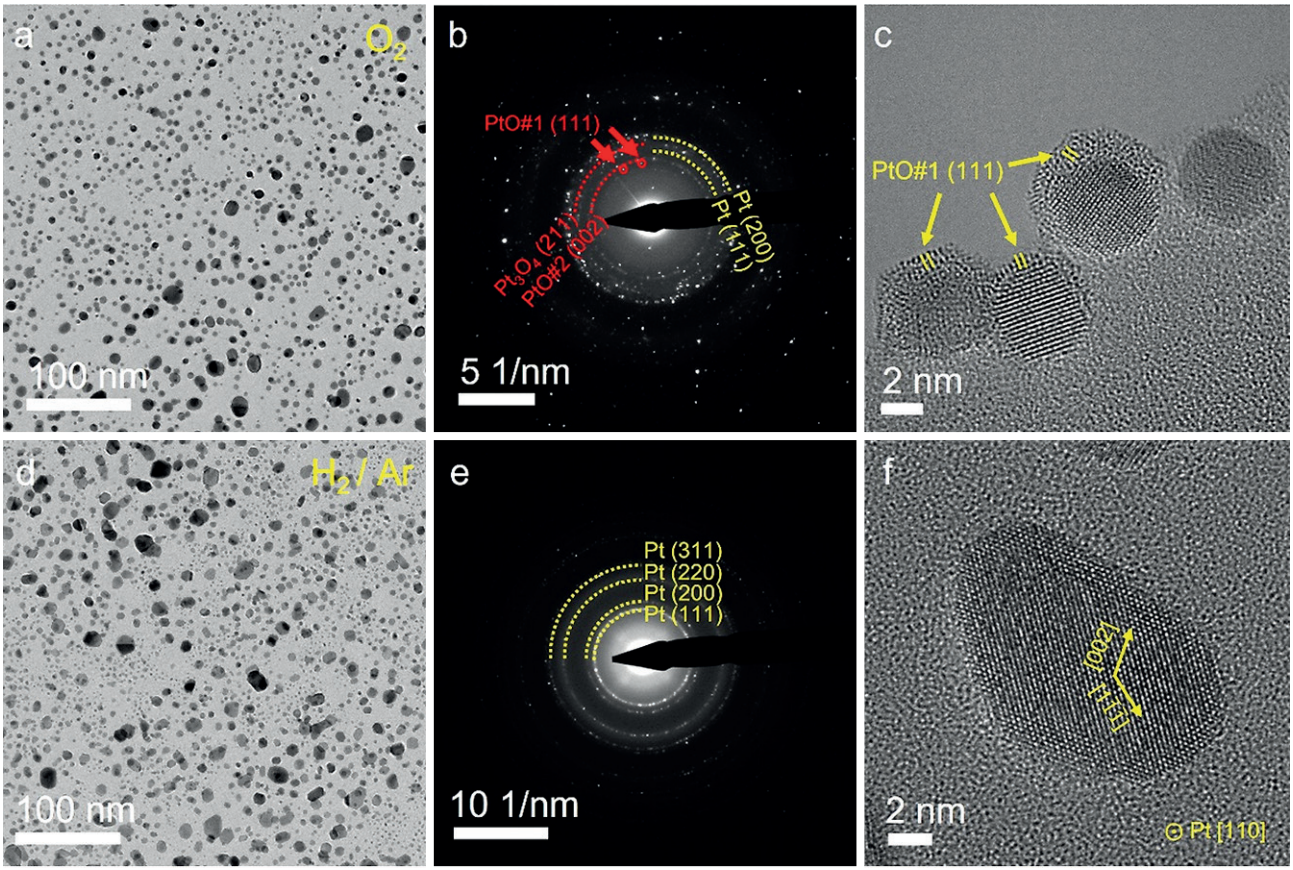

Fig. 4. **Atomic structures of Pt nanocrystals annealed for 2 hours in oxidizing (a-c) and reducing atmosphere (d–f). Low-magnification TEM images (a, d) and corresponding SAED patterns (b, e), and HRTEM images (c, f) exhibit the distinct size, structures, and morphologies of nanocrystals annealed in different atmospheres.**

the 2 hours of heating. This is possible that the preceding formation of a thin layer of PtO_x blocked the progress of their coalescence.

After heating for 2 hours in a reducing gas environment, the Pt nanocrystals exhibited a specific shape morphology with smooth and flat exposed crystal surfaces, as shown in Fig. 4d. The SAED in Fig. 4e reveals a pure Pt phase formed under the reaction condition. The HRTEM image shows clear lattice fringes and confirms a single crystal structure of Pt nanocrystal along the [110] crystal direction (Fig. 4f).

DISCUSSION

The size stability of Pt nanocrystals in the reaction condition or operational environment depends on many factors, including the temperature, atmosphere, and also the supported substrates. Here the SiN_x film was selected as the supporting substrate of Pt nanocrystals because of the chemical stableness and inertness which may impose negligible effects on the nanocrystal coarsening process. In this case, we can figure out more reliable influences of the atmosphere. Our results demonstrated that the size of Pt nanocrystal is more stable under an O_2 environment than in the H_2/Ar environment. This is due to the formation of a thin PtO_x layer in an oxygen environment that could prevent nanocrystals migration and coalescence, even though their thickness is only a few atomic layers. This effect may arise from several reasons: (i) the PtO_x probably has strong interaction with the SiN_x film that greatly reduces the particle mobility; (ii) the PtO_x has a variety of crystal phases that lead to the difficulty of coalescence; (iii) the PtO_x shell also weakens the interaction between different Pt nanocrystals.

CONCLUSION

The Pt nanocrystal with uniform size can be prepared by e-beam reduction and thermal decomposition of solid-state H_2PtCl_6 precursor. The size stability of Pt nanocrystals was in-situ investigated under O_2 and H_2/Ar environments at the temperature of 300°C. The formation of PtO_x shell could effectively reduce the particle migration, coalescence and aggregation phenomena, and thus improve the size stability of Pt nanocrystal. Such an in-situ investigation method can provide a new pathway to investigate the size stability of nanocrystals, which will benefit the design, fabrication, and application of nanocrystals.

REFERENCES

1. Tang, M.; Yuan, W.; Ou, Y.; Li, G.; You, R.; Li, S.; Yang, H.; Zhang, Z.; Wang, Y. Recent Progresses on Structural Reconstruction of Nanosized Metal Catalysts via Controlled-Atmosphere Transmission Electron Microscopy: A Review. *Acs Catal.* 2020: 10 (24): 14419-14450. https://doi.org/10.1021/acscatal.0c03335.

2. Roldan Cuenya, B. Metal nanoparticle catalysts beginning to shape-up. *Acc Chem Res.* 2013: 46 (8): 1682-1691. https://doi.org/10.1021/ar300226p.

3. Calle-Vallejo, F.; Loffreda, D.; Koper, M. T.; Sautet, P. Introducing structural sensitivity into adsorption-energy scaling relations by means of coordination numbers. *Nat Chem.* 2015: 7 (5): 403-410. https://doi.org/10.1038/nchem.2226.

4. Cao, S.; Tao, F. F.; Tang, Y.; Li, Y.; Yu, J. Size- and shape-dependent catalytic performances of oxidation and reduction reactions on nanocatalysts. *Chem Soc Rev.* 2016: 45 (17): 4747-4765. https://doi.org/10.1039/c6cs00094k.

5. Haruta, M. Size- and support-dependency in the catalysis of gold. *Catal Today.* 1997: 36 (1): 153-166. https://doi.org/10.1016/s0920-5861(96)00208-8.

6. Tao, F. F.; Crozier, P. A. Atomic-Scale Observations of Catalyst Structures under Reaction Conditions and during Catalysis. *Chem Rev.* 2016: 116 (6): 3487-3539, Review. https://doi.org/10.1021/cr5002657.

7. Behafarid, F.; Roldan Cuenya, B. Towards the Understanding of Sintering Phenomena at the Nanoscale: Geometric and Environmental Effects. *Top Catal.* 2013: 56 (15-17): 1542-1559. https://doi.org/10.1007/s11244-013-0149-4.

8. Bartholomew, C. H. Mechanisms of catalyst deactivation. *Applied Catalysis A: General.* 2001: 212 (1-2): 17-60. https://doi.org/10.1016/s0926-860x(00)00843-7.

9. Haruta, M. Catalysis of Gold Nanoparticles Deposited on Metal Oxides. *Cattech.* 2002: 6 (3): 102-115. https://doi.org/10.1023/a:1020181423055.

10. Reece, C.; Redekop, E. A.; Karakalos, S.; Friend, C. M.; Madix, R. J. Crossing the great divide between single-crystal reactivity and actual catalyst selectivity with pressure transients. *Nature Catalysis.* 2018: 1 (11): 852-859. https://doi.org/10.1038/s41929-018-0167-5.

11. Hansen, T. W.; Delariva, A. T.; Challa, S. R.; Datye, A. K. Sintering of catalytic nanoparticles: particle migration or Ostwald ripening? *Acc Chem Res.* 2013: 46 (8): 1720-1730. https://doi.org/10.1021/ar3002427.

12. Yaguchi, T.; Kanemura, T.; Shimizu, T.; Imamura, D.; Watabe, A.; Kamino, T. Development of a technique for in situ high temperature TEM observation of catalysts in a highly moisturized air atmosphere. *J Electron Microsc (Tokyo)*. 2012: 61 (4): 199-206. https://doi.org/10.1093/jmicro/dfs041.

13. He, B.; Zhang, Y.; Liu, X.; Chen, L. In-situ Transmission Electron Microscope Techniques for Heterogeneous Catalysis. *Chemcatchem*. 2020: 12 (7): 1853-1872. https://doi.org/10.1002/cctc.201902285.

14. Zhu, C.; Liang, S.; Song, E.; Zhou, Y.; Wang, W.; Shan, F.; Shi, Y.; Hao, C.; Yin, K.; Zhang, T.; et al. In-situ liquid cell transmission electron microscopy investigation on oriented attachment of gold nanoparticles. *Nat Commun*. 2018: 9 (1): 421. https://doi.org/10.1038/s41467-018-02925-6.

15. Yuan, W.; Zhang, D.; Ou, Y.; Fang, K.; Zhu, B.; Yang, H.; Hansen, T. W.; Wagner, J. B.; Zhang, Z.; Gao, Y.; et al. Direct In Situ TEM Visualization and Insight into the Facet-Dependent Sintering Behaviors of Gold on TiO_2. *Angew Chem Int Ed Engl*. 2018: 57 (51): 16827-16831. https://doi.org/10.1002/anie.201811933.

16. Zhu, Y.; Zhao, H.; He, Y.; Wang, R. In-situ transmission electron microscopy for probing the dynamic processes in materials. *Journal of Physics D: Applied Physics*. 2021: 54 (44). https://doi.org/10.1088/1361-6463/ac1a9d.

17. Ye, H.; Yang, F.; Sun, Y.; Wang, R. Atom-Resolved Investigation on Dynamic Nucleation and Growth of Platinum Nanocrystals. *Small Methods*. 2022: e2200171. https://doi.org/10.1002/smtd.202200171.

18. Simonsen, S. B.; Chorkendorff, I.; Dahl, S.; Skoglundh, M.; Sehested, J.; Helveg, S. Ostwald ripening in a Pt/SiO_2 model catalyst studied by in situ TEM. *J Catal*. 2011: 281 (1): 147-155. https://doi.org/10.1016/j.jcat.2011.04.011.

19. Wang, S.; Sawada, H.; Chen, Q.; Han, G. G. D.; Allen, C.; Kirkland, A. I.; Warner, J. H. In Situ Atomic-Scale Studies of the Formation of Epitaxial Pt Nanocrystals on Monolayer Molybdenum Disulfide. *Acs Nano*. 2017: 11 (9): 9057-9067. https://doi.org/10.1021/acsnano.7b03648.

20. Jiang, Y.; Wang, Y.; Zhang, Y. Y.; Zhang, Z. F.; Yuan, W. T.; Sun, C. H.; Wei, X.; Brodsky, C. N.; Tsung, C. K.; Li, J. X.; et al. Direct observation of Pt nanocrystal coalescence induced by electron-excitation-enhanced van der Waals interactions. *Nano Res*. 2014: 7 (3): 308-314. https://doi.org/10.1007/s12274-013-0396-5.

21. Li, L.; Wang, L. L.; Johnson, D. D.; Zhang, Z.; Sanchez, S. I.; Kang, J. H.; Nuzzo, R. G.; Wang, Q.; Frenkel, A. I.; Li, J.; et al. Noncrystalline-to-crystalline transformations in Pt nanoparticles. *J Am Chem Soc*. 2013: 135 (35): 13062-13072. https://doi.org/10.1021/ja405497p.

INFORMATION ABOUT THE AUTHORS

Qinglin Liu, Bachelor of Science in Physics, University of Science and Technology Beijing, School of Mathematics and Physics, Beijing, China, s20190793@xs.ustb.edu.cn

Huanyu Ye, Bachelor of Science in Physics, University of Science and Technology Beijing, School of Mathematics and Physics, Beijing, China, b20180341@xs.ustb.edu.cn

Zhihong Zhang, Doctor of Philosophy in Physics, Assistant Professor, Beijing Key Laboratory for Magneto-Photoelectrical Composite and Interface Science, Institute for Multidisciplinary Innovation, University of Science and Technology Beijing, Beijing, China, zhzhang@ustb.edu.cn

Rongming Wang, Doctor of Philosophy in Physics, Professor, Beijing Advanced Innovation Center for Materials Genome Engineering, Beijing Key Laboratory for Magneto-Photoelectrical Composite and Interface Science, Institute for Multidisciplinary Innovation, School of Mathematics and Physics, University of Science and Technology Beijing, Beijing, China, rmwang@ustb.edu.cn

CONTRIBUTION OF THE AUTHORS

The authors contributed equally to this article.

The authors declare no conflicts of interests.

The article was submitted 10.05.2022; approved after reviewing 03.06.2022; accepted for publication 07.06.2022.